Food Chemistry 194 (2016) 712–722

Contents lists available at ScienceDirect

Food Chemistry

journal homepage: www.elsevier.com/locate/foodchem

Adsorption properties of macroporous adsorbent resins for separation of anthocyanins from mulberry

Yao Chen [a,1], Weijie Zhang [b,1], Ting Zhao [b], Fang Li [c], Min Zhang [b], Jing Li [d], Ye Zou [e], Wei Wang [e], Samuel J. Cobbina [a], Xiangyang Wu [a,*], Liuqing Yang [b,*]

[a] School of the Environment and Safety, Jiangsu University, 301 Xuefu Rd., 212013 Zhenjiang, Jiangsu, China
[b] School of Chemistry and Chemical Engineering, Jiangsu University, 301 Xuefu Rd., 212013 Zhenjiang, Jiangsu, China
[c] School of Medicine, Jiangsu University, 301 Xuefu Rd., 212013 Zhenjiang, Jiangsu, China
[d] School of Pharmacy, Jiangsu University, 301 Xuefu Rd., 212013 Zhenjiang, Jiangsu, China
[e] School of Food and Biological Engineering, Jiangsu University, 301 Xuefu Rd., 212013 Zhenjiang, Jiangsu, China

ARTICLE INFO

Article history:
Received 9 March 2015
Received in revised form 31 July 2015
Accepted 20 August 2015
Available online 21 August 2015

Chemical compounds studies in this article:
Cyanidin-3-glucoside (PubChem CID: 12303203)
Cyanidin-3-rutinoside (PubChem CID: 29231)
Cyanidin (PubChem CID: 128861)
Hexose (PubChem CID: 169005)
Rutinose (PubChem CID: 441429)
Methanol (PubChem CID: 887)
Ethanol (PubChem CID: 702)
Ammonium sulfate (PubChem CID: 6097028)
Acetic acid (PubChem CID: 176)
Muriatic acid (PubChem CID: 313)

Keywords:
Mulberry anthocyanins
Macroporous resin
Separation
Identification
Adsorption mechanism

ABSTRACT

In this study, the adsorption/desorption characteristics of mulberry anthocyanins (MA) on five types of macroporous resins (XAD-7HP, AB-8, HP-20, D-101 and X-5) were evaluated, XAD-7HP and AB-8 showed higher adsorption/desorption capacities. On the basis of static adsorption test, XAD-7HP and AB-8 resins were selected for kinetics, isotherms and thermodynamics. The adsorption mechanism indicated that the process was better explained by pseudo-first-order kinetics and the Langmuir isotherm model, and the thermodynamics tests showed that the processes were exothermic, spontaneous and thermodynamically feasible. Dynamic tests were performed on a column packed with XAD-7HP and AB-8, and breakthrough volume was reached at 15 and 14 bed volumes of MA solution, respectively. The purity of the fraction by 40% ethanol elution on XAD-7HP reached 93.6%, from which cyanidin-3-glucoside and cyanidin-3-rutinoside were identified by HPLC–ESI-MS/MS. The method could be used to prepare high purity anthocyanins from mulberry fruits as well as other plants.

1. Introduction

In the past decades, there has been increased interest in diets containing berries because of the potential health benefits derived from the biological effects of the anthocyanins they contain (Gardana, Ciappellano, Marinoni, Fachechi, & Simonetti, 2014). Anthocyanins have been proven to be good antioxidant compounds due to their effective free radical scavenging properties and their potential use as dietary modulators for various diseases (Grigoras, Destandau, Zubrzycki, & Elfakir, 2012; He & Giusti, 2010).

Mulberry (*Morus alba* L.) is a traditional Chinese fruit; it serves as a rich source of anthocyanins and has been widely consumed in food processed products and effectively applied in folk medicines (Chang et al., 2013). As a bioactive phytochemical, anthocyanins extracted from mulberries are typically known as nutraceuticals due to their excellent antioxidant capacity. In virtue of such characteristics, anthocyanins provide protective effects against chronic

* Corresponding authors.
E-mail addresses: wuxy@ujs.edu.cn (X. Wu), yangliuqing@ujs.edu.cn (L. Yang).
[1] Contributed to this article equally and are co-first authors.

http://dx.doi.org/10.1016/j.foodchem.2015.08.084
0308-8146/

diseases such as diabetes, cancer and cardiovascular diseases (Liang, Wu, Zhu, et al., 2012; Yin & Chao, 2008). Moreover, they have been shown to have health-promoting properties in neuroprotective, analgesic and anti-inflammatory activities (Chen et al., 2006; Zhao, Sheng, Zheng, & Liu, 2011). Our previous study also showed that mulberry anthocyanins (MA) possess good antioxidant activity *in vivo* (Liang, Wu, Zhao, et al., 2012) and neuroprotective effects on mice (Chen, Li, et al., 2014). Other studies have also demonstrated that MA can exhibit inhibitory effects on the migration and invasion of human lung cancer cell lines (Oki et al., 2006). The mulberry fruit extract, by its antioxidant and anti-apoptotic effects, significantly protected neurons against neurotoxins *in vitro* and *in vivo* Parkinson's disease (PD) models (Kim et al., 2010). Therefore, the mulberry fruit could be a type of potential functional food to protect against many types of diseases.

Despite their significant potential, mulberries have been rarely used in the medicine industry. They are usually made into juices and fruit wines, or even consumed directly. As a result of the low yields achieved during extraction and the instability of anthocyanins, high-purity anthocyanin products are still unavailable in the market. Hence, the preparation of pure anthocyanins from mulberries is a very promising endeavor, if technologically challenging (Santos, Albarelli, Beppu, & Meireles, 2013).

The separation of anthocyanins from plants has been studied using high-speed counter-current chromatography (HSCCC) (Sheng et al., 2014), preparative high-performance liquid chromatography (HPLC) (Wang, Yin, Xu, & Liu, 2014), solid-phase extraction (SPF) (Santos et al., 2014) and so on. However, these methods are fraught with several disadvantages, in that they are time-consuming, laborious, expensive with poor recovery, and unsuitable for large-scale industrial production. Accordingly, macroporous resin emerges as an alternative candidate for the separation of anthocyanins from plant materials. First, the material is easily obtained and lost cost. In addition, the utilization of macroporous resin always reveals outstanding properties, including good selectivity, high mechanical strength, and fast adsorption speed. Moreover, macroporous resin as an efficient adsorbent has received fruitful advancements in academia, including cyaniding-3-O-glucoside from orange juice (Scordino, Di Mauro, Passerini, & Maccarone, 2004), anthocyanins from citrus-processing by-products (Di Mauro, Arena, Fallico, Passerini, & Maccarone, 2002), anthocyanins from blueberries (Wang et al., 2014), and anthocyanins from blood oranges (Cao, Pan, Yao, & Fu, 2010).

In this study, five macroporous resins were selected according to their polarity and separation effects in previous studies (Chandrasekhar, Madhusudhan, & Raghavarao, 2012; Jampani, Naik, & Raghavarao, 2014). In these studies, the resins were used to systematically investigate the adsorption and desorption of anthocyanins from mulberry extract and develop a simple, efficient, and eco-friendly process for the separation and purification of MA with the optimal resin.

2. Materials and methods

2.1. Chemicals, reagents and adsorbents

Standard of cyaniding-3-O-glucosid was purchased from J&K Chemical Co., Ltd. (Shanghai, China). All solvent and chemicals used were of analytical grade or HPLC grade.

2.2. Pretreatment of macroporous resins

Macroporous resins including AB-8, D101, and X-5 were provided by the Chemical Plant of Naikai University (Tianjin, China). Amberlite XAD-7HP and HP 20 were purchased from Sigma–Aldrich Chemical Co. (St. Louis, MO, USA) and Mitsubishi Chemical Co. (Tokyo, Japan), respectively. The physical properties of these resins are summarized in Table 1a. Prior to the study, adsorbent was activated by overnight treatment with 2 bed volumes (BV) of 95% ethanol for the removal of monomers and porogenic agents trapped inside the pores during the synthesis process. This was done until there was no residue after distillation, and further rinsed by 4–5 BV distilled water until neutral.

2.3. Preparation of crude anthocyanins extracts from mulberry

2.3.1. Pretreatment of mulberry fruits

Mulberry fruits, were manually picked at the ripening stage on the farm of Sericultural Research Institute (Jiangsu University of Science and Technology, Zhenjiang, Jiangsu, China), and then transported to laboratory immediately, and stored in polyethylene bags at −18 °C in a refrigerator until analysis.

2.3.2. Extraction of crude mulberry anthocyanins

Aqueous two-phase extraction was applied to extract MA according to the method published by our previous studies (Wu et al., 2011). The defrosted mulberry fruit (10 g) was triturated, homogenized and treated with an aqueous two-phase system consisting of 30% (w/w) ethanol, and 20% (w/w) ammonium sulfate. The residue was dissolved with 1 L of 0.1% HCl acidified 70% (v/v) ethanol and extracted for 24 h. This process was repeated until the filtrate became light-colored. The supernatant was then concentrated to a volume by a rotary evaporator to remove the ethanol at temperatures not exceeding 40 °C for 1 h, and then freeze-dried.

2.3.3. Determination of anthocyanin content

The total anthocyanins content in extracts was directly determined using the pH differential method (Hosseinian, Li, & Beta, 2008). The absorbance of anthocyanin was measured at 513 nm and 700 nm, employing Eq. (1):

$$\text{Anthocyanins concentrations (mg/L)} = \frac{A \times M\omega \times DF}{\varepsilon \times L} \quad (1)$$

where $A = \left[(A_{513} - A_{700})_{\text{pH1.0}} - (A_{513} - A_{700})_{\text{pH4.5}}\right]$, $M\omega$ is the molecular weight of anthocyanins (449.2 g/mol); DF is the dilution factor; ε is the molar extinction coefficient (26,900 L/cm mol); L is the path length (1 cm).

2.4. Static adsorption and desorption tests

2.4.1. Static adsorption and desorption properties of the resins

Activated adsorbent (2.0 g dry weight) was added to 10 mL of anthocyanins extract in 100 mL flask while agitating on a vibratory shaker at 25 °C for 12 h to reach the adsorption equilibrium. After adsorption, filtration was completed, and the filtrate was subjected to further analysis. After reaching the adsorption equilibrium, the resin was washed with deionized water for 2–3 times and then desorbed with 20 mL 80% ethanol in a 100 mL flask while agitating on a vibratory shaker at 25 °C for 30 min to reach the desorption equilibrium. The content of anthocyanins was then measured using the pH differential method.

The adsorption capacity was quantified as follows:

$$Q_e = \frac{(C_0 - C_e) \times V_i}{W} \quad (2)$$

$$Q_{re} = (C_0 - C_e)/C_o \times 100\% \quad (3)$$

where C_0 and C_e are the initial and equilibrium concentrations of anthocyanins in the solution, respectively (mg/mL); Q_e represents the adsorption capacity at adsorption equilibrium (mg/g dry resin);

Table 1a
Physical and chemical properties of the tested resins.

Trade name	Polarity	Particle diameter (mm)	Surface area (m^2/g)	Average pore dimeter (nm)
XAD-7HP	Weak-polar	0.6	500	20–60
AB-8	Weak-polar	1.13–1.17	480–520	75–110
HP-20	Non-polar	0.3–1.25	600	290
D101	Non-polar	0.3–1.25	600	13–14
X-5	Polar	0.3–1.25	160–200	250–290

V_i is the volume of the initial sample solution (mL); W is the dry weight of the tested resins (g); Q_{re} (%) is the adsorption ratio.

The desorption capacity was quantified as follows:

$$Q_d = \frac{C_d V_d}{W} \tag{4}$$

$$D = \frac{C_d V_d}{(C_0 - C_e)V_i} \times 100\% \tag{5}$$

where C_d is the concentration of solutes in the desorption equilibrium solution (mg/mL); Q_d is the desorption capacity after desorption equilibrium (mg/g dry resin); V_d is the volume of the desorption solution (mL); D (%) is the desorption ratio; C_0, C_e, V_i and W are the same as described above.

2.4.2. Adsorption kinetics on the selected resins

Pre-treated resin (2.0 g) was mixed with 10 mL of MA extracts solution in a flask and placed in a water shaker (120 rpm) at room temperature. An aliquot of supernatant was obtained every 40 min for the first 12 h. Adsorption kinetics were evaluated by the pseudo-fist and pseudo-second-order model, which were tested to predict the mechanism involved in the adsorption process (Ho, 2006). Triplicate experiments were performed.

Pseudo-first-order model:

$$Q_t = Q_e - Q_e e^{-k_1 t} \tag{6}$$

Pseudo-second-order model:

$$Q_t = \frac{k_2 Q_e^2 t}{1 + k_2 Q_e t} \tag{7}$$

where k_1 and k_2 are the rate constant of the pseudo-first and pseudo-second-order models, respectively; Q_e (mg/g) is the adsorptive capacity at equilibrium; Q_t (mg/g) is the concentration of anthocyanins absorbed at time t.

2.4.3. Adsorption isotherms on the selected resins

The adsorption isotherms on the selected resins at various temperatures were analyzed by varying the initial concentration of anthocyanin extracts, which were investigated by contacting 10 mL of extracting solutions at different concentrations with pre-weighed amounts of hydrated resins (equal to 2.0 g dry resin) on an incubation shaker (120 rpm) at 25, 30 and 35 °C, respectively. The concentrations of anthocyanin extracts were set at 3.0, 4.0, 5.0, 6.0, 7.0 and 8.0 mg/mL. Langmuir and Freundlich equations were evaluated to analyze their degrees of fitness (Deng, Jia, Luo, & Li, 2014). Triplicate experiments were performed.

The Langmuir model can be expressed by the following mathematical formula:

$$Q_e = \frac{Q_m K_L C_e}{1 + K_L C_e} \tag{8}$$

Langmuir Eq. (8) can be linearized as follows:

$$\frac{C_e}{Q_e} = \frac{1}{K_L Q_m} + \frac{C_e}{Q_m} \tag{9}$$

where K_L is the association Langmuir constant; Q_e (mg/g) is the adsorption capacity at equilibrium; C_e (mg/mL) is the concentration of solute in solution at equilibrium; Q_m (mg/g) is the maximum adsorptive capacity, theoretically.

The Freundlich model is widely applied for many different adsorbate/adsorbent systems for liquid and gas phase adsorption with a two-parameter, which can be expressed by the following formula:

$$Q_e = K_F C_e^{\frac{1}{n}} \tag{10}$$

A linearized formula of Freundlich can be expressed as:

$$\ln Q_e = \ln K_F + \frac{1}{n} \ln C_e \tag{11}$$

where K_F is the Freundlich constant that measures the adsorption capacity; $1/n$ is an empirical constant that reflects the magnitude of the adsorption driving force.

2.4.4. Adsorption thermodynamics on the selected resins

Adsorption thermodynamics can reflect the in-depth information regarding structural and inherent energy change of adsorbents after adsorption. They also provide the mechanism involved in the adsorption process (Chen, Yang, et al., 2014). Enthalpy change can be calculated using the Clausius–Clapeyron equation, which can be linearized as:

$$\ln K_c = \frac{\Delta S^\circ}{R} - \frac{\Delta H^\circ}{RT} \tag{12}$$

The Gibbs free energy change can be calculated as follows:

$$\Delta G^\circ = -RT \ln K_c \tag{13}$$

where ΔH° (kJ/mol) is enthalpy change; ΔS° (J mol^{-1} K^{-1}) is entropy change; ΔG° (kJ mol^{-1} K^{-1}) is Gibbs free energy change; R (8.314 J mol^{-1} K^{-1}) is the ideal gas constant; T (K) is the temperature; K_c is the equilibrium distribution coefficient, which is the ratio of the amount adsorbed on the solid to the equilibrium concentration in solution.

2.5. Dynamic adsorption and desorption tests

A glass column (1.6 cm × 50 cm) was loaded with the selected resins (XAD-7HP and AB-8) with a resin bed of 10 mL.

2.5.1. Optimization of the adsorption flow rate and loading amount

The optimal adsorption flow rate was evaluated by comparing the flow rate of 1.0, 1.5, 2.0 and 2.5 mL/min, the effluent were collected at 5 min interval, and analyzed with a UV–VIS spectrophotometer at 520 nm.

2.5.2. Optimization of the eluent

The loading of the sample solution was stopped, once reaching the adsorption equilibrium. The column was washed with 3 BV deionized water firstly, and then eluted with a series of ethanol solutions (20%, 40%, 60%, 80%, 100% (v/v) ethanol solutions containing 0.1% HCl, respectively), and a series of the selected ethanol solution with different pH (3.0, 4.0, 5.0, 6.0 and 7.0). The flow rate was set at 1.5 mL/min. The eluted aliquots were collected every 5 min, and measured with a UV–VIS spectrophotometer at 520 nm.

2.5.3. Optimization of the desorption flow rate

The desorption flow rate of the optimal elution solution was evaluated by comparing the elution flow rate, which was set at 1.0, 1.5, and 2.0 mL/min, respectively. The eluted aliquots were

Table 1b
Static adsorption and desorption capacities of anthocyanins on the five kinds of resins.

	Q_e (mg/g)	Q_{re} (%)	Q_d (mg/g)	D (%)
X-5	2.98 ± 0.25	77.36 ± 5.8	2.14 ± 0.21	71.72 ± 3.7
XAD-7HP	3.57 ± 0.20*	86.45 ± 5.6	2.89 ± 0.15*	80.81 ± 3.7
AB-8	3.59 ± 0.19*	86.92 ± 4.3	2.79 ± 0.18	77.86 ± 4.2
HP 20	3.10 ± 0.23	78.10 ± 5.2	2.47 ± 0.20	79.71 ± 4.9
D 101	3.01 ± 0.16	76.69 ± 4.6	2.00 ± 0.12	66.49 ± 5.1

**$P < 0.01$, compared with X-5 resin.
* $P < 0.05$, compared with X-5 resin.

collected every 5 min, and analyzed with a UV–VIS spectrophotometer at 520 nm.

2.6. Isolation and purification of MA

The crude extract was dissolved in distilled water and passed through a pretreatment resins column (1.6 cm × 30 cm). The column was first eluted with a volume of 4–5 BV distilled water to remove the majority of sugars, organic acids, proteins and ions, and then eluted of anthocyanins by different concentrates of

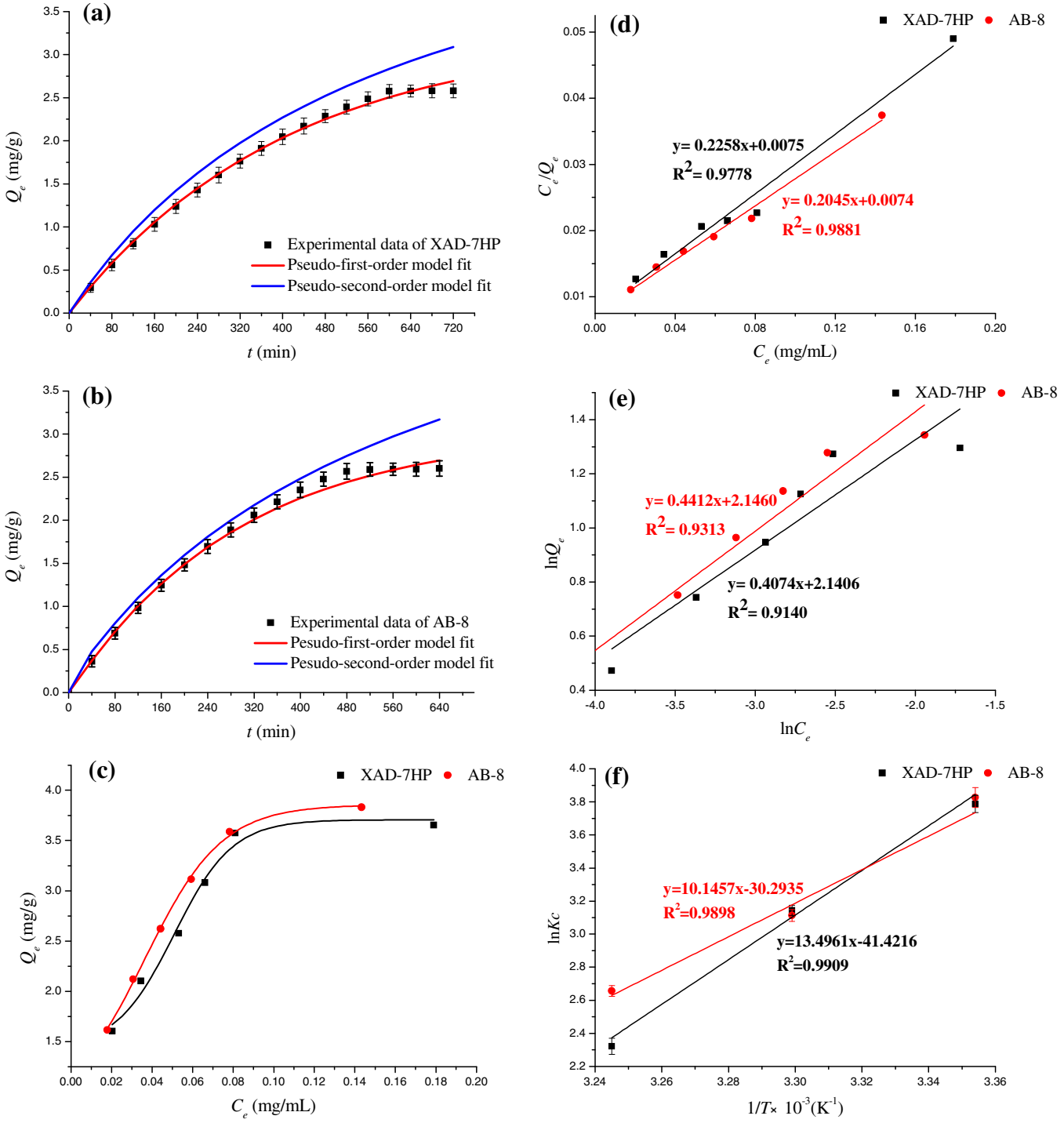

Fig. 1. Adsorption mechanism on XAD-7HP and AB-8 resins. (a) Adsorption kinetics curve and modeling of XAD-7HP; (b) adsorption kinetics curve and modeling of AB-8; (c) adsorption isotherms at 25 °C; (d) Langmuir model at 25 °C; (e) Freundlich model at 25 °C; (f) adsorption thermodynamics based on Eq. (12).

Table 2a
Kinetic parameters of MA onto XAD-7HP and AB-8 resins.

	Q_e (mg/g)	Pseudo-first-order model			Pseudo-second-order model		
		R^2	$Q_{e,c}$ (mg/g)	k_1 (L/min)	R^2	$Q_{e,c}$ (mg/g)	k_2 (g/(mg min))
XAD-7HP	3.57	0.9942	3.54	2.47×10^{-3}	0.9687	5.63	3.00×10^{-4}
AB-8	3.59	0.9873	3.61	3.42×10^{-3}	0.9861	5.88	2.93×10^{-4}

Table 2b
Adsorption isotherms equation and parameters of MA on XAD-7HP and AB-8 resins at different temperatures.

	T (°C)	Langmuir				Freundlich			
		Equation	R^2	K_L	Q_m (mg/g)	Equation	R^2	K_F	$1/n$
XAD-7HP	25	$C_e/Q_e = 0.2258C_e + 0.0075$	0.9778	30.11	4.4287	$Q_e = 8.5045C_e^{0.4074}$	0.9140	8.5045	0.4074
	30	$C_e/Q_e = 0.2279C_e + 0.0168$	0.9829	13.57	4.3879	$Q_e = 7.7207C_e^{0.4832}$	0.9346	7.7207	0.4832
	35	$C_e/Q_e = 0.2435C_e + 0.0449$	0.9276	5.42	4.1068	$Q_e = 7.7383C_e^{0.6665}$	0.9551	7.5383	0.6665
AB-8	25	$C_e/Q_e = 0.2045C_e + 00074$	0.9881	27.63	4.8900	$Q_e = 8.5506C_e^{0.4412}$	0.9313	8.5506	0.4412
	30	$C_e/Q_e = 0.2090C_e + 0.0170$	0.9680	12.29	4.7847	$Q_e = 8.0221C_e^{0.4990}$	0.9059	8.0221	0.4990
	35	$C_e/Q_e = 0.2500C_e + 0.0208$	0.9756	12.02	4.0000	$Q_e = 5.3844C_e^{0.4089}$	0.9415	5.3844	0.4089

Table 2c
Thermodynamic parameters of XAD-7HP and AB-8 on the sorption process.

	T (°C)	$\Delta S°$ (J mol^{-1} K^{-1})	$\Delta H°$ (kJ mol^{-1})	$\Delta G°$ (kJ mol^{-1})
XAD-7HP	25	−344.38	−112.21	−9.39
	30			−7.67
	35			−6.60
AB-8	25	−251.19	−84.35	−9.48
	30			−7.85
	35			−6.81

acidified ethanol solution (20%, 40%, 60%, 80% (v/v) ethanol solutions containing 0.1% HCl, respectively). The separated fractions were collected, concentrated and lyophilized to dryness.

2.7. Recovery of anthocyanins with selected resin column chromatography

The recovery of anthocyanins was determined by calculating the amount of anthocyanins in powered extract before and after purification on column packed with the selected resins to evaluate the efficiency of the method. The equation of recovery was described by the following mathematical formula:

$$\text{Recovery yield } (\%) = \frac{\text{the amount of MA after column}}{\text{the amount of MA before column}} \times 100\% \quad (14)$$

2.8. Regeneration and reusability on selected resin column chromatography

The feasibility of regenerating resins (XAD-7HP and AB-8) to repeated use was investigated. After first use, the resin was soaked with 4% NaOH solution (v/v), 4% HCl solution (v/v), and absolute ethyl alcohol, successively, and then washed by volume of distilled water for several times until becoming natural, so that the adsorption/desorption capacity of resin could be determined again. The equation for recovery by reusability can also be described by Eq. (14).

2.9. HPLC–ESI-MS/MS analysis

The HPLC–ESI-MS/MS system adopted in this work consisted of Agilent 1200 system (Thermo Fisher Scientific, America), equipped with a quaternary pump, surveyor plus detector and linear ion trap mass spectrometer detector LXQ (Thermo Mod. Finnigan™ LXQ™). Chromatographic separation was performed using a Hypersil ODS column (Φ 4.6 × 250 mm, 5 μm, Dalian, China). Sample was filtrated through a syringe filter (0.45 μm), 10 μL of filtrates was injected. The mobile phase consisted of 2% (v/v) acetic acid in water (solvent A) and 100% methanol (solvent B) at a flow rate of 1.0 mL/min. The gradient elution programme was performed as follows: 0–14 min, 32–70% B; 15–30 min, 70% B. The column temperature was maintained at 30 °C and the detection wavelength was 520 nm. The MS/MS parameters were as follows: positive mode; ESI source voltage, 5.0 kV; capillary voltage, 36 V; sheath gas flow rate, 40 arb; aux gas flow rate, 5 arb; sweep gas flow rate, 0 arb; capillary temperature, 300 °C; and scan range, 50–1200 m/z.

2.10. Statistical analyses

Data were expressed as mean ± SD values. Statistical analysis was performed by using SPSS 16.0. Significance of the differences between variables was tested by one-way ANOVA. P values less than 0.05 was considered statistically significant.

3. Results and discussion

3.1. Static adsorption and desorption capacities

Static adsorption and desorption capacities of anthocyanins on the five types of resins are depicted in Table 1b. Compared with X-5, the adsorption capacities of XAD-7HP is significantly higher than that of X-5 ($^*P < 0.05$), which is the same as AB-8. XAD-7HP and AB-8 had the highest adsorption ratios of 86.45% and 86.92%, respectively, which could be attributed to their similarity to the polarity of anthocyanins (Jampani et al., 2014). AB-8 showed the highest adsorption capacity (3.59 mg/g), followed by XAD-7HP at 3.57 mg/g. The slightly low adsorption capacity of XAD-7HP may be explained by its smaller pore size and surface area than that of AB-8. Previous research suggests that the surface area along with pore size were the decisive factors reflecting the adsorption capacity (Chandrasekhar et al., 2012).

In the desorption tests, the desorption capacities of XAD-7HP was significantly higher than that of X-5 ($^*P < 0.05$) compared with X-5. Polarity was one of the most significant variables that affected the desorption capacity of resin. In other words, the higher the polarity of resin, the weaker the desorption capacity (Buran et al., 2014). However, static tests indicated overall that XAD-7HP and AB-8 were consistently more efficient at adsorption and desorption than the other three resins, and hence they were chosen for further tests.

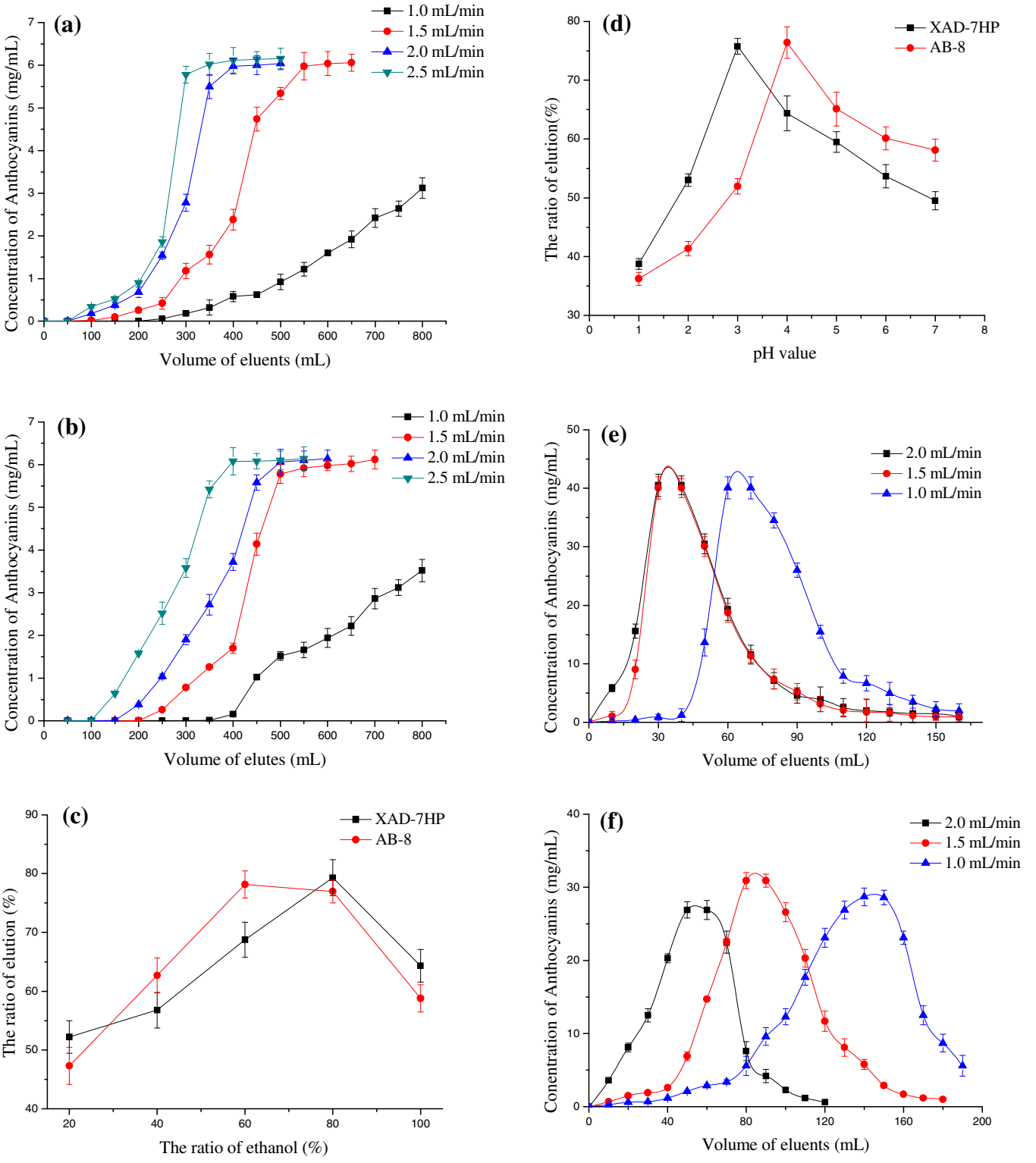

Fig. 2. (a and b) Dynamic adsorption curves of total anthocyanins on XAD-7HP and AB-8 resins at different flow rates; (c) effect of different ethanol ratios on elution capacity on XAD-7HP and AB-8 resins; (d) effect of different pH values on elution capacity on XAD-7HP and AB-8 resins; (e and f) dynamic desorption curves of total anthocyanins on XAD-7HP and AB-8 resins at different flow rates; (g) the elution curve of XAD-7HP resins; (h) the elution curve of AB-8 resins.

3.2. Adsorption kinetics on the selected resins

Adsorption kinetics describes the adsorption rate of the adsorbate on an adsorbent and the adsorption time from the beginning to equilibrium. The reaction rate of the adsorbate uptake is required for selecting optimum operating conditions for the full-scale batch process and can be evaluated by adsorption kinetics studies. Both pseudo-first and pseudo-second-order models have been applied for adsorption kinetics studies. The pseudo-first-order model is generally applicable over the initial stage of an

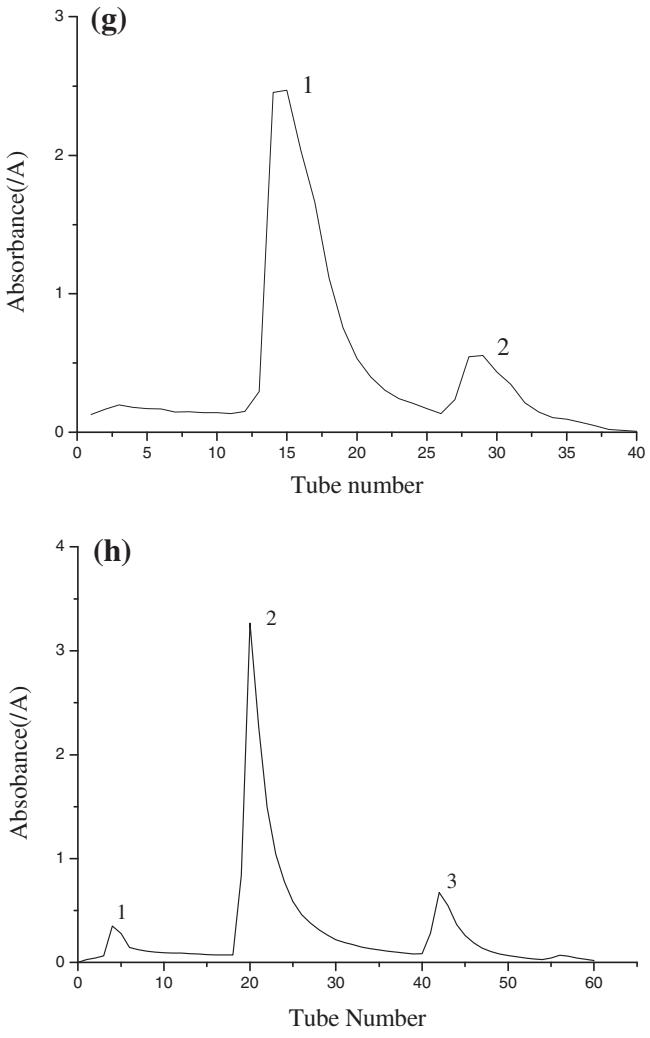

Fig. 2 (*continued*)

Table 3
The recovery of primary and regeneration resins.

	Fractions	Primary Recovery (%)	Regeneration Recovery (%)
XAD-7HP	Fraction 1 (eluted by 40% ethanol)	39.63	36.82
	Fraction 2 (eluted by 60% ethanol)	22.41	17.16
	Total recovery	62.04	53.98
AB-8	Fraction 1 (eluted by 20% ethanol)	9.77	7.34
	Fraction 2 (eluted by 40% ethanol)	33.14	28.36
	Fraction 3 (eluted by 60% ethanol)	8.04	6.82
	Total recovery	50.95	42.52

adsorption process, while the pseudo-second-order model assumes that the rate-limiting step is chemisorption and predicts the behavior over the whole range of adsorption (Chang et al., 2012). The adsorption kinetics of anthocyanins on XAD-7HP and AB-8 resins were shown in Fig. 1(a), (b) and Table 2a.

Fig. 1(a) shows that the adsorption of MA on XAD-7HP increased rapidly at the first 320 min and then increased slowly until equilibrium at approximately 560 min. Moreover, the adsorption rate constants and liner regression values from two kinetic equations were summarized in Table 2a. R^2 for the pseudo-first-order kinetic model (0.9942) was better than that of the pseudo-second-order kinetic model (0.9687). The pseudo-first-order kinetic model calculated value ($Q_{e,c}$, 3.54 mg/g) was also close to the experimental data (Q_e, 3.57 mg/g). The results showed that the pseudo-first-order model gave a better fit to the kinetic adsorption data of MA onto XAD-7HP. As shown in Fig. 1(a) and Table 2a, the same results were observed for AB-8. Similar observations were made in previous studies using resins on different compounds (Chen & Zhang, 2014; Sandhu & Gu, 2013).

3.3. Adsorption isotherms on the selected resins

Adsorption isotherms described the relationship between the equilibrium adsorption capacity of adsorbate adsorbed onto adsorbent and the equilibrium concentration of adsorbate in liquid at a constant temperature. The adsorption isotherms of MA onto XAD-7HP and AB-8 resins at 25 °C, 30 °C and 35 °C are summarized in Table 2b, and the adsorption isotherms at the optimum temperature is presented in Fig. 1(c).

The adsorption capacity of XAD-7HP and AB-8 of MA (Fig. 1(c)) increased rapidly at lower mulberry extract concentration and then approached equilibrium slowly. However, the adsorption capacity of MA was found to decrease following a rise in temperature from 25 °C to 30 °C. The results suggested that the adsorption processes of MA onto XAD-7HP and AB-8 were exothermic in nature, which were in conformity with the results of the thermodynamic studies.

To establish the optimum model, the experimental equilibrium data were fit into two isotherm models: the Langmuir and Freundlich models.

3.3.1. Langmuir equation

The Langmuir isotherm model, shown in Fig. 1(d), described the monolayer adsorption onto a homogeneous surface with no interaction between adjacent adsorbed molecules (Huang, Sun, Wang, Yue, & Yang, 2011). The correlation coefficients of the Langmuir equation for MA on XAD-7HP and AB-8 resins were above 0.97 and 0.98, respectively. The high correlation coefficients indicated that the models were suitable for describing the tested adsorption system in the concentration range studied. K_L is the Langmuir constant, the values of K_L indicate whether the isotherm is favorable ($0 < K_L < 1$), linear ($K_L = 1$), or unfavorable ($K_L > 1$). The values of K_L at different temperatures summarized in Table 2b suggested that the isotherm of XAD-7HP and AB-8 were favorable.

3.3.2. Freundlich equation

Compared with the Langmuir isotherm model, the Freundlich isotherm model reflects the adsorption process on a heterogeneous surface and is suitable to describe adsorption in a narrow range of solute concentration (Gao, Yu, Yue, & Quek, 2013). The Freundlich isotherm models about MA onto XAD-7HP and AB-8 at 25 °C are presented in Fig. 1(e). The linear plot of $\ln Q_e$ and $\ln C_e$ suggested that the applicability of the Freundlich adsorption isotherm as the correlation coefficient was high. K_F is a Freundlich affinity parameter for a hetero-disperse system, n is related to the magnitude, which is related to the sorption driving force and the energy distribution of the sorption sites, and the value of $1/n$ indicates the type of isotherm (Chen & Zhang, 2014). Adsorption can take place easily when the value of $1/n$ is between 0.1 and 0.5, but when the value of $1/n$ is between 0.5 and 1, it is difficult for adsorption to occur. Furthermore, adsorption occurs with difficulty if the $1/n$ value exceeds 1 (Vasiliu, Bunia, Racovita, & Neagu, 2011). As shown in Table 2b, the values of $1/n$ reflected that the adsorption of MA on XAD-7HP and AB-8 were both favorable at the selected temperature, indicating that the adsorption of MA on XAD-7HP and AB-8 resins could take place easily. The results obtained from the

Freundlich adsorption isotherm provided further confirmation of the exceptional promise in the separation of this compound for both the selected resins.

3.4. Adsorption thermodynamics on the selected resins

To understand the sorption process from the aspect of energy change, three basic thermodynamic constants were chosen in the thermodynamic analysis, which were shown in Table 2c and Fig. 1(f). ΔH° was determined through the slope of $\ln K_c$ versus $1/T$, ΔG° and ΔS° also could be calculated by using Eqs. (12) and (13).

The negative ΔH° value demonstrated the exothermic nature of MA adsorption onto XAD-7HP and AB-8 resins (Cheng, Jin, Gao, Xia, & Chen, 2013). It suggested that the initial adsorption occur on the active sites with a low value of ΔH°. During the adsorption process, the active sites decrease, and further adsorption became more difficult with a high value of ΔH°. The values of ΔH° were less than 40 kJ/mol where physical adsorption was expected to be the dominating mechanism (Gao et al., 2013). As chemical adsorption was not the main process, it was anticipated that both resins would not stand any structural changes during the adsorption process. This is up to the specifications made by the Codex Alimentarius Commission, as fruit juice production should only be conducted through physical methods to avoid any chemical interaction with juice components during processing (Qiu, Guo, & Chang, 2007).

The values of ΔG° were found to be negative at all temperatures, suggesting that the sorption of MA on XAD-7HP and AB-8 resins were both spontaneous and thermodynamically feasible (Yousef, El-Eswed, & Al-Muhtaseb, 2011). Meanwhile, the ΔG° values of AB-8 were similar to that of XAD-7HP, indicating that XAD-7HP and AB-8 favored the sorption of MA.

In addition, ΔS° was also determined to be negative, showing that the randomness of the adsorption process decreased at the solid–liquid interface, which occurs due to the anthocyanin molecules being firmly adsorbed onto the surface of the resins (Duran, Ozdes, Gundogdu, & Senturk, 2011).

3.5. Dynamic adsorption and desorption curves on the selected resins

3.5.1. Optimization of the adsorption flow rate and loading amount

The dynamic leakage curves of MA on XAD-7HP and AB-8 resins were obtained on the volume of effluent liquid and the absorbance of eluents herein. As shown in Fig. 2(a) and (b), the higher the loading flow rate was, the faster the increase of the amount of MA in leak solution. Meanwhile, the higher flow rate would provide a higher adsorption efficiency in a short time; however, as adsorption time increased, the accumulative adsorption ratio using the higher flow rate remained approximately constant. The flow rates of XAD-7HP and AB-8 were both set at 1.5 mL/min; under this condition, the processing volume of the MA solution on the two resins were approximately 450 and 500 mL, respectively.

3.5.2. Optimization of the eluent

To understand the effect of ethanol concentration and pH on the elution of anthocyanins, studies have been carried out with acidified aqueous solution, and the results are shown in Fig. 2 (c) and (d). As shown in Fig. 2(c), for XAD-7HP resin, the elution capacity increased before the ratio of ethanol reached 80%, but AB-8 resin just reached 60%.

The effects of eluent (80% and 60% ethanol for XAD-7HP and AB-8, respectively) on desorption capacity at different pH values were studied. As presented in Fig. 2(d), the elution capacity of XAD-7HP resin towards MA linearly increased with increasing pH value of 80% ethanol solution from 1.0 to 3.0, while AB-8 resin is from 1.0 to 4.0. With the results above, the MA behaves as a weak acid according to the presence of phenolic hydroxyl groups, and the solubility of MA increases with increasing pH. However, the molecular structures of all types of anthocyanins are similar just with different substituent groups; as a result, their solubility increased with increasing pH, so a different concentration of ethanol solution with 0.1% HCl was selected. It was rational to employ 80% and 60% ethanol with 0.1% HCl as the main eluent of XAD-7HP and AB-8 resin, respectively.

3.5.3. Optimization of the dynamic desorption flow rate

To effectively elute MA from the resins, a proper flow rate is necessary. As presented in Fig. 2(e) and (f), the desorption processes of XAD-7HP and AB-8 under different flow rates successively reached their plateaus after the consumption of the eluent. It is obvious that, when XAD-7HP and AB-8 resins reached the flow rate of 2.0 mL/min and 1.5 mL/min, respectively, they both could afford the best desorption capacity per unit volume of eluent.

3.6. Isolation and purification of mulberry anthocyanins

To isolate high-purity anthocyanin mixtures and monomers from mulberries, this study successively eluted anthocyanins by different concentrations of acidified ethanol solution (20%, 40%, 60%, 80% (v/v) ethanol solutions containing 0.1% HCl, respectively). The eluted fractions were shown in Fig. 2(g) and (h). There were two fractions for XAD-7HP and three fractions for AB-8.

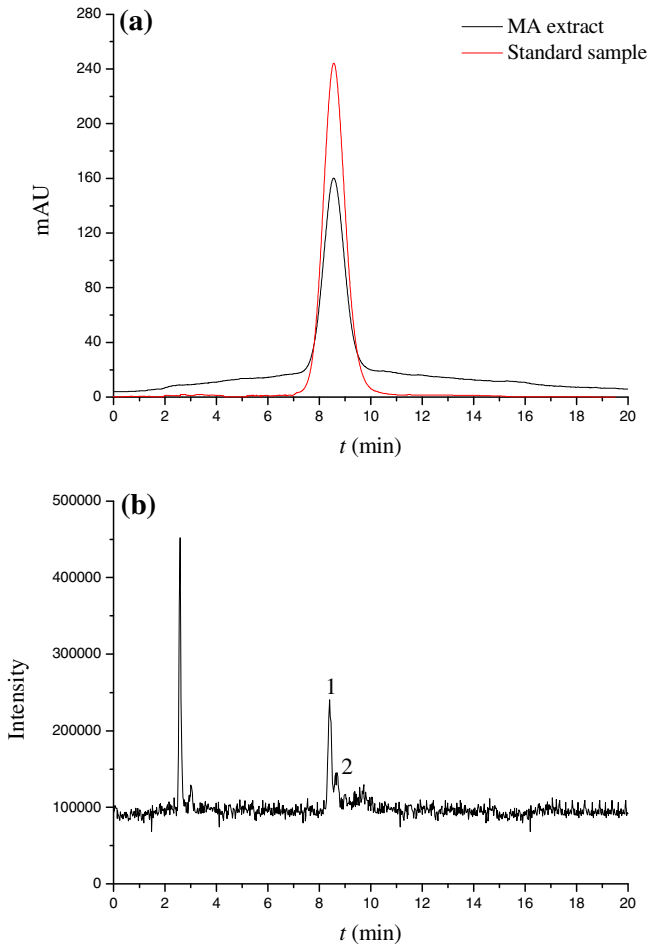

Fig. 3. (a) Analytical HPLC–ESI-MS/MS chromatograms of standard sample and MA extract at 520 nm; (b) the ESI full mass chromatogram of the MA extract; (c–f) the mass spectra of component 1 and 2 of the full mass chromatogram.

(c) Component 1: +MS (449)

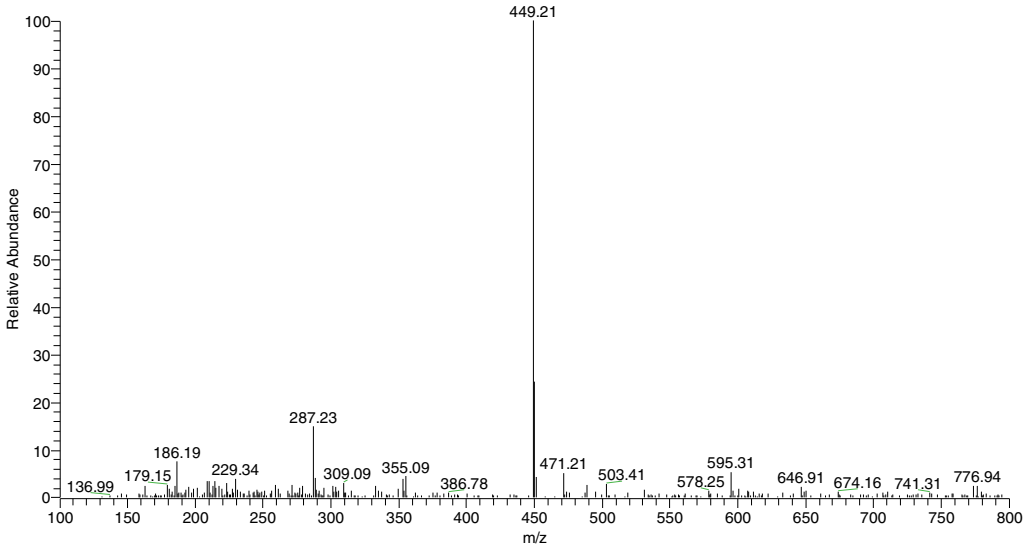

(d) Component 1: +MS^2 (287)

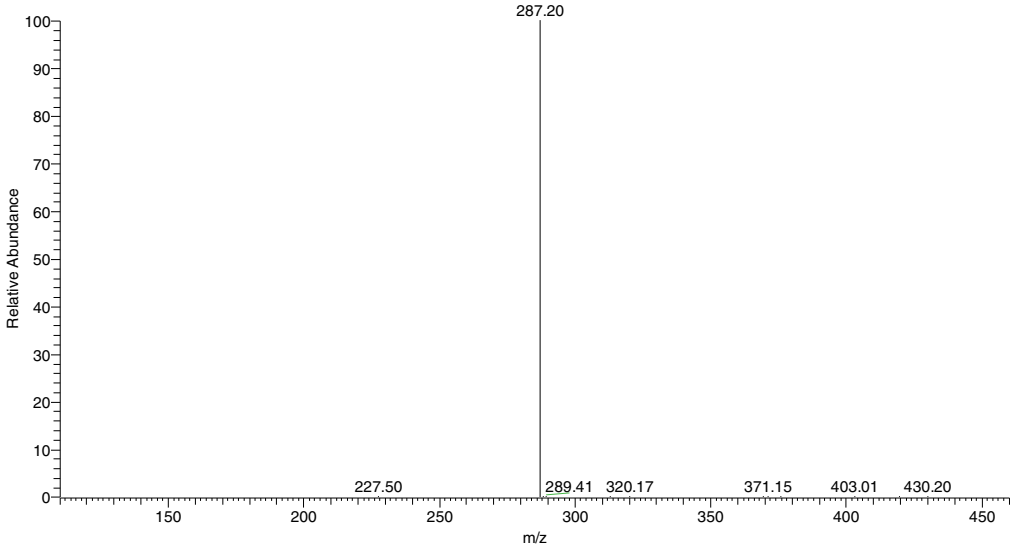

Fig. 3 (*continued*)

The dynamic adsorption and desorption tests were triplicate under optimal conditions, and the percent recovery of MA was calculated by Eq. (14). After the treatment of XAD-7HP and AB-8 resins, the recovery of different fractions was summarized in Table 3. The recovery of regenerated resins was similar to the primary resins. This demonstrated that both XAD-7HP and AB-8 resins had high reusability and were perfect sorbent for anthocyanin purification from mulberry fruits.

3.7. HPLC–ESI-MS/MS analysis

The highest purity fraction of the 5 fractions eluted from XAD-7HP and AB-8 resins was the 40% XAD-7HP elution fraction, as the purity of the fraction could reach 93.6% with a recovery of 39.63%. To understand the basic structure as well as the structural stability of anthocyanins, the chemical structures were determined by HPLC–ESI-MS/MS, and the results are shown in Fig. 3. The major anthocyanin peaks in the highest purity fraction were identified by comparing the retention times of the standards, the m/z of each anthocyanin molecule, and the fragmentation patterns with the previous value (Barnes, Nguyen, Shen, & Schug, 2009).

Component 1 (retention time (t_R) = 8.33 min) produced a molecular ion at m/z 449 and a fragment ion at 287, indicating that it is a cyanidin derivative. The neutral loss of 162 mass units corresponded to a hexose molecule. Hence, component 1 tentatively identified as cyaniding-3-glucoside. Component 2 (t_R = 8.49 min) revealed a molecular ion at m/z 595 and a MS^2 fragment at 287; the neutral loss of 308 mass units corresponded to a rutinose. As a result, the component was in conformity with cyaniding-3-rutinoside. This result was in agreement with our previous studies (Liang, Wu, Zhu, et al., 2012; Wu et al., 2011) and other published studies (Pawlowska, Oleszek, & Braca, 2008; Wu et al., 2013) that determined that cyaniding-3-glucoside and cyaniding-3-

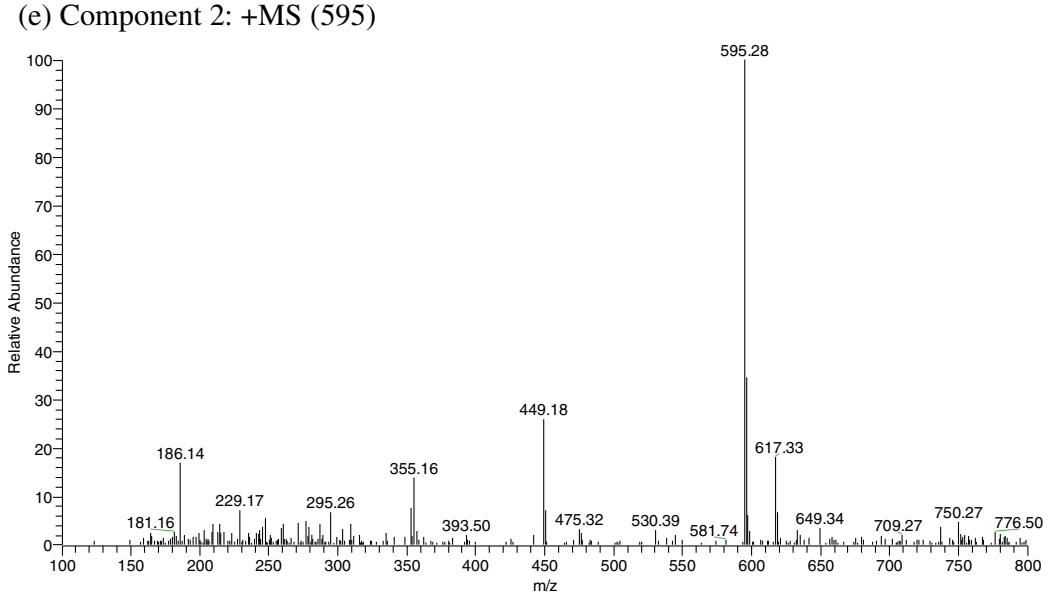

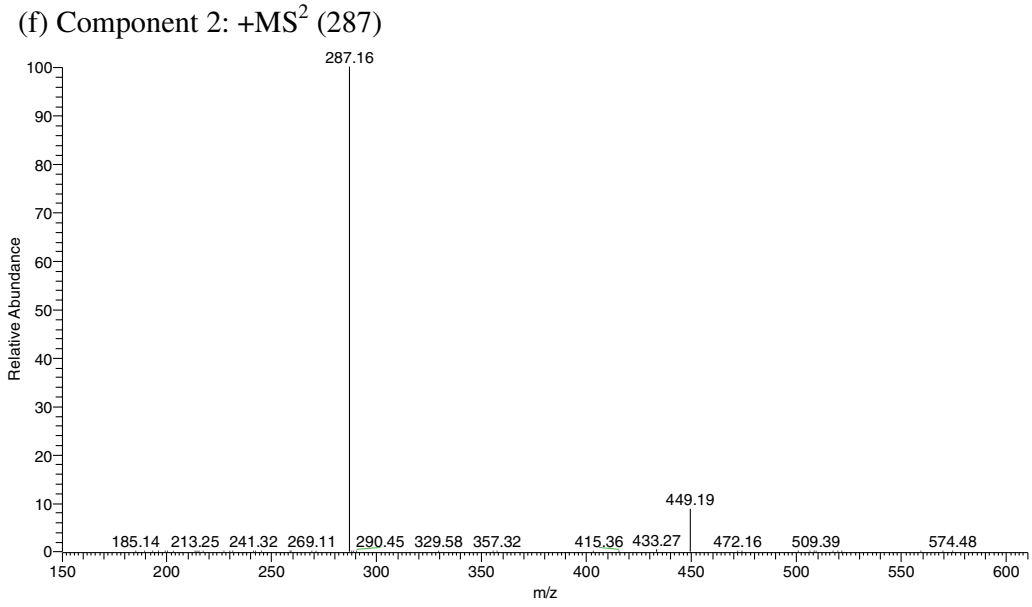

Fig. 3 (*continued*)

rutinoside are the two main components in mulberry (*M. alba* L.) fruits.

4. Conclusions

In conclusion, this study has provided insights into the separation and purification of anthocyanins from mulberry extract using an adsorbent (Amberlite XAD-7HP). XAD-7HP showed higher adsorption/desorption capacities and ratios than other resins. The adsorption capacity was 3.57 mg/g, while the ratios of adsorption and desorption were 86.45% and 80.81%, respectively. The pseudo-first-order model and Langmuir isotherm model were suitable to describe the process of adsorption of MA from mulberry fruits. In the investigation of adsorption thermodynamics, the negative value of ΔG° and ΔH° indicated that the process was spontaneous and exothermic. Hence, the adsorption process was controlled by a physical mechanism rather than a chemical mechanism. The purity of the fraction by 40% ethanol elution on XAD-7HP reached 93.6%, from which cyanidin-3-glucoside and cyanidin-3-rutinoside were identified by HPLC–ESI-MS/MS. The results reflected the advantages of the method, which are environmental friendliness, procedural simplicity, lower cost and high efficiency. The results also present a valuable and practical strategy for separating high-purity anthocyanins and help to promote the purification of anthocyanins from mulberry fruits as well as from other plant.

Acknowledgments

This study was financially supported by National Natural Science Foundation of China (31371733) and Graduate Innovative Projects in Jiangsu Province (KYLX15_1090). The authors are thankful to Professor Weiguo Zhao (Key Laboratory of Silkworm Biotechnology, Ministry of Agriculture, Sericultural Research

Institute, Chinese Academy of Agricultural Sciences, Zhenjiang, Jiangsu, China) for providing us with mulberry samples and their identification.

References

Barnes, J. S., Nguyen, H. P., Shen, S., & Schug, K. A. (2009). General method for extraction of blueberry anthocyanins and identification using high performance liquid chromatography–electrospray ionization-ion trap-time of flight-mass spectrometry. *Journal of Chromatography A, 1216*(23), 4728–4735.

Buran, T. J., Sandhu, A. K., Li, Z., Rock, C. R., Yang, W. W., & Gu, L. (2014). Adsorption/desorption characteristics and separation of anthocyanins and polyphenols from blueberries using macroporous adsorbent resins. *Journal of Food Engineering, 128*, 167–173.

Cao, S.-q., Pan, S.-y., Yao, X.-l., & Fu, H.-f. (2010). Isolation and purification of anthocyanins from blood oranges by column chromatography. *Agricultural Sciences in China, 9*(2), 207–215.

Chandrasekhar, J., Madhusudhan, M. C., & Raghavarao, K. S. M. S. (2012). Extraction of anthocyanins from red cabbage and purification using adsorption. *Food and Bioproducts Processing, 90*(C4), 615–623.

Chang, J.-J., Hsu, M.-J., Huang, H.-P., Chung, D.-J., Chang, Y.-C., & Wang, C.-J. (2013). Mulberry anthocyanins inhibit oleic acid induced lipid accumulation by reduction of lipogenesis and promotion of hepatic lipid clearance. *Journal of Agricultural and Food Chemistry, 61*(25), 6069–6076.

Chang, X.-L., Wang, D., Chen, B.-Y., Feng, Y.-M., Wen, S.-H., & Zhan, P.-Y. (2012). Adsorption and desorption properties of macroporous resins for anthocyanins from the calyx extract of roselle (*Hibiscus sabdariffa* L.). *Journal of Agricultural and Food Chemistry, 60*(9), 2368–2376.

Chen, P.-N., Chu, S.-C., Chiou, H.-L., Kuo, W.-H., Chiang, C.-L., & Hsieh, Y.-S. (2006). Mulberry anthocyanins, cyanidin 3-rutinoside and cyanidin 3-glucoside, exhibited an inhibitory effect on the migration and invasion of a human lung cancer cell line. *Cancer Letters, 235*(2), 248–259.

Chen, R., Yang, Q., Zhong, Y., Li, X., Liu, Y., Li, X.-M., ... Zeng, G.-M. (2014a). Sorption of trace levels of bromate by macroporous strong base anion exchange resin: Influencing factors, equilibrium isotherms and thermodynamic studies. *Desalination, 344*, 306–312.

Chen, Y., Li, Q., Zou, Y., Zhou Zhao, X., Feng Wei, W., Bao Yong, T., ... Wu Xiang, Y. (2014). Protective effect of mulberry extract against Pb-induced learning and memory deficits in mice. *Biomedical and Environmental Sciences, 27*(1), 70–75.

Chen, Y., & Zhang, D. (2014). Adsorption kinetics, isotherm and thermodynamics studies of flavones from *Vaccinium bracteatum* thunb leaves on NKA-2 resin. *Chemical Engineering Journal, 254*, 579–585.

Cheng, Y.-M., Jin, X.-H., Gao, D., Xia, H.-F., & Chen, J.-H. (2013). Thermodynamics and kinetics of lysozyme adsorption onto two kinds of weak cation exchangers. *Biotechnology and Bioprocess Engineering, 18*(5), 950–955.

Deng, T., Jia, J., Luo, N., & Li, H. (2014). A dual-task method for the simultaneous detoxification and enrichment of stilbene glycoside from Polygonum multiflorum roots extract by macroporous resin. *Chemical Engineering Journal, 237*, 138–145.

Di Mauro, A., Arena, E., Fallico, B., Passerini, A., & Maccarone, E. (2002). Recovery of anthocyanins from pulp wash of pigmented oranges by concentration on resins. *Journal of Agricultural and Food Chemistry, 50*(21), 5968–5974.

Duran, C., Ozdes, D., Gundogdu, A., & Senturk, H. B. (2011). Kinetics and isotherm analysis of basic dyes adsorption onto almond shell (*Prunus dulcis*) as a low cost adsorbent. *Journal of Chemical and Engineering Data, 56*(5), 2136–2147.

Gao, Z. P., Yu, Z. F., Yue, T. L., & Quek, S. Y. (2013). Adsorption isotherm, thermodynamics and kinetics studies of polyphenols separation from kiwifruit juice using adsorbent resin. *Journal of Food Engineering, 116*(1), 195–201.

Gardana, C., Ciappellano, S., Marinoni, L., Fachechi, C., & Simonetti, P. (2014). Bilberry adulteration: Identification and chemical profiling of anthocyanins by different analytical methods. *Journal of Agricultural and Food Chemistry, 62*(45), 10998–11004.

Grigoras, C. G., Destandau, E., Zubrzycki, S., & Elfakir, C. (2012). Sweet cherries anthocyanins: An environmental friendly extraction and purification method. *Separation and Purification Technology, 100*, 51–58.

He, J., & Giusti, M. M. (2010). Anthocyanins: Natural colorants with health-promoting properties. In: M. P. Doyle, & T. R. Klaenhammer (Eds.), *Annual Review of Food Science and Technology* (pp. 163–187) (Vol. 1).

Ho, Y.-S. (2006). Review of second-order models for adsorption systems. *Journal of Hazardous Materials, 136*(3), 681–689.

Hosseinian, F. S., Li, W., & Beta, T. (2008). Measurement of anthocyanins and other phytochemicals in purple wheat. *Food Chemistry, 109*(4), 916–924.

Huang, L., Sun, Y., Wang, W., Yue, Q., & Yang, T. (2011). Comparative study on characterization of activated carbons prepared by microwave and conventional heating methods and application in removal of oxytetracycline (OTC). *Chemical Engineering Journal, 171*(3), 1446–1453.

Jampani, C., Naik, A., & Raghavarao, K. S. M. S. (2014). Purification of anthocyanins from jamun (*Syzygium cumini* L.) employing adsorption. *Separation and Purification Technology, 125*, 170–178.

Kim, H. G., Ju, M. S., Shim, J. S., Kim, M. C., Lee, S.-H., Huh, Y., ... Oh, M. S. (2010). Mulberry fruit protects dopaminergic neurons in toxin-induced Parkinson's disease models. *British Journal of Nutrition, 104*(1), 8–16.

Liang, L., Wu, X., Zhao, T., Zhao, J., Li, F., Zou, Y., ... Yang, L. (2012). In vitro bioaccessibility and antioxidant activity of anthocyanins from mulberry (*Morus atropurpurea* Roxb.) following simulated gastro-intestinal digestion. *Food Research International, 46*(1), 76–82.

Liang, L., Wu, X., Zhu, M., Zhao, W., Li, F., Zou, Y., & Yang, L. (2012). Chemical composition, nutritional value, and antioxidant activities of eight mulberry cultivars from China. *Pharmacognosy Magazine, 8*(31), 215–224.

Oki, T., Kobayashi, M., Nakamura, T., Okuyama, M., Masuda, M., Shiratsuchi, H., & Suda, I. (2006). Changes in radical-scavenging activity and components of mulberry fruit during maturation. *Journal of Food Science, 71*(1), C18–C22.

Pawlowska, A. M., Oleszek, W., & Braca, A. (2008). Quali-quantitative analyses of flavonoids of *Morus nigra* L. and *Morus alba* l. (Moraceae) fruits. *Journal of Agricultural and Food Chemistry, 56*(9), 3377–3380.

Qiu, N., Guo, S., & Chang, Y. (2007). Study upon kinetic process of apple juice adsorption de-coloration by using adsorbent resin. *Journal of Food Engineering, 81*(1), 243–249.

Sandhu, A. K., & Gu, L. (2013). Adsorption/desorption characteristics and separation of anthocyanins from muscadine (*Vitis rotundifolia*) juice pomace by use of macroporous adsorbent resins. *Journal of Agricultural and Food Chemistry, 61*(7), 1441–1448.

Santos, D. T., Albarelli, J. Q., Beppu, M. M., & Meireles, M. A. A. (2013). Stabilization of anthocyanin extract from jabuticaba skins by encapsulation using supercritical CO_2 as solvent. *Food Research International, 50*(2), 617–624.

Santos, V. d. S., Bisen-Hersh, E., Yu, Y., Ribeiro Cabral, I. S., Nardini, V., Culbreth, M., ... Aschner, M. (2014). Anthocyanin-rich acai (*Euterpe oleracea* Mart.) extract attenuates manganese-induced oxidative stress in rat primary astrocyte cultures. *Journal of Toxicology and Environmental Health – Part A – Current Issues, 77*(7), 390–404.

Scordino, M., Di Mauro, A., Passerini, A., & Maccarone, E. (2004). Adsorption of flavonoids on resins: Cyanidin 3-glucoside. *Journal of Agricultural and Food Chemistry, 52*(7), 1965–1972.

Sheng, F., Wang, Y., Zhao, X., Tian, N., Hu, H., & Li, P. (2014). Separation and identification of anthocyanin extracted from mulberry fruit and the pigment binding properties toward human serum albumin. *Journal of Agricultural and Food Chemistry, 62*(28), 6813–6819.

Vasiliu, S., Bunia, I., Racovita, S., & Neagu, V. (2011). Adsorption of cefotaxime sodium salt on polymer coated ion exchange resin microparticles: Kinetics, equilibrium and thermodynamic studies. *Carbohydrate Polymers, 85*(2), 376–387.

Wang, E., Yin, Y., Xu, C., & Liu, J. (2014). Isolation of high-purity anthocyanin mixtures and monomers from blueberries using combined chromatographic techniques. *Journal of Chromatography A, 1327*, 39–48.

Wu, T., Qi, X., Liu, Y., Guo, J., Zhu, R., Chen, W., ... Yu, T. (2013). Dietary supplementation with purified mulberry (*Morus australis* Poir) anthocyanins suppresses body weight gain in high-fat diet fed C57BL/6 mice. *Food Chemistry, 141*(1), 482–487.

Wu, X., Liang, L., Zou, Y., Zhao, T., Zhao, J., Li, F., & Yang, L. (2011). Aqueous two-phase extraction, identification and antioxidant activity of anthocyanins from mulberry (*Morus atropurpurea* Roxb.). *Food Chemistry, 129*(2), 443–453.

Yin, M.-c., & Chao, C.-y. (2008). Anti-campylobacter, anti-aerobic, and anti-oxidative effects of roselle calyx extract and protocatechuic acid in ground beef. *International Journal of Food Microbiology, 127*(1–2), 73–77.

Yousef, R. I., El-Eswed, B., & Al-Muhtaseb, A. a. H. (2011). Adsorption characteristics of natural zeolites as solid adsorbents for phenol removal from aqueous solutions: Kinetics, mechanism, and thermodynamics studies. *Chemical Engineering Journal, 171*(3), 1143–1149.

Zhao, X., Sheng, F., Zheng, J., & Liu, R. (2011). Composition and stability of anthocyanins from purple *Solanum tuberosum* and their protective influence on Cr(VI) targeted to bovine serum albumin. *Journal of Agricultural and Food Chemistry, 59*(14), 7902–7909.